International Research Journal of Engineering and Technology (IRJET) e-ISSN: 2395 -0056
Volume: 04 Issue: 04 | Apr -2017 www.irjet.net p-ISSN: 2395-0072

SIMULATION OF PASSENGER CAR BY ATTACHING ADD-ON DEVICE TO REDUCE DRAG FORCE BY CFD APPROACH

Shashank Arya[1], Pankaj Goud[1], Vishal Sharma[1], Shubham Mathur[1], Sourabh Tripathi[1], Vishal Shukla[2]

[1] *Research Scholar, Department of Mechanical Engineering, IITM College, Gwalior*

[2] *Assistant professor, Mechanical Department , IITM College, Gwalior- 475001, Madhya pradesh*

Abstract - *As we know the consequence of drag force over a car is increasing due to better conditions of road which leads the driver to drive a car fastly, as the car runs fastly on highway the amount of air resistance increases .this increased resistance relatively rising the fuel consumption The Research is about the simulation of passenger car by using add-on devices to reduce drag force by computational fluid dynamics (CFD) approach. A passenger car prototype is firstly prepared in CATIA software and this prototype is imported in Hyper mesh Fluent for further investigation of drag coefficient, the three aspectal computational analysis was carried out using with the help of software tools like ANSYS-CFX to simulate the flow of air around the automobiles , CFD code were used to run the simulation. The main purpose of the study is to predict the drag coefficient and lift coefficient computationally. Several factors that influence the drag coefficient such as flow separation, vortex, effect of pressure coefficient, Detail velocity profile and pressure distribution plots around the car envelopes have been presented.*

Key Words: *Drag & lift force, Coefficient, virtual wind tunnel, prototype of passenger car, ANSYS-CFX, Hyper mesh fluent, spoilers, spline , tail-plate, VGs*

1.INTRODUCTION

"Aerodynamics" is a stem of fluid dynamics concerned with studying the movement of air, predominantly when it interacts with a moving object . Understanding the motion of air (often called a flow field) around an object enables the estimate of forces and moments acting on the object. Typical properties considered for a flow field consist of velocity, pressure, density and temperature as a function of position and time[1]. Airflow over a vehicle determines the drag forces, which in turn affects the car's performance and efficiency testing equipment has been designed to measure both the vertical and horizontal components of air resistance on a prototype car. When a car goes faster and faster the weight of the car changes due to air resistance. Depending on the direction (upward or downward) this is called either lift or down force, respectively. The horizontal component, the drag of the prototype of car will be measured. Drag is the amount of force that the air is pushing on the car at a certain speed[2]. Aerodynamics and its analysis are basically divided into two major sub-categories, namely the exterior and interior aerodynamics. Exterior aerodynamics is the study of flow around solid objects of various shapes. On the other hand, Interior aerodynamics is the study of flow through passages in solid objects[1]. If air resistance can be minimized, the car will be more efficient because less energy is lost to friction[2]. Today, car designers is keen to show their designing skills over the external face of a vehicle to reduce drag force by attaching add-on devices such as spoiler, VGs, tail-plates, splines, diffuser on the body of car and these devices do not worsening the design of a car & increase its efficiency. Investigation of aerodynamic drag can be done experimentally by wind tunnel experiment and computational numerical simulation by cfd technique and software was used ANSYS FLUENT and Altair's virtual wind tunnel, leveraging Acusolve's CFD technology. In this paper our numerical analysis was done by cfd technology on software to cut drag force on passenger car using add-on devices spoiler, diffuser, VGs, tail plates etc. A more elaborate description of CFd technology is given below :

2. HOW TO UTILIZE CFD SIMULATION IN VEHICLE AERODYNAMICS & STEPS

Computational fluid dynamics (CFD) is one of the branches of fluid mechanics that uses numerical methods and algorithms to solve and analyze problems that involve fluid flows. Computers are used to simulate the contact of liquids and gases with Faces defined by boundary conditions. Computational Fluid Dynamic codes are prearranged around the numerical algorithms that can tackle fluid flow problems. All the CFD codes available in the market have three basic elements which split the complete analysis of the numerical experiment to be performed on the specific domain or geometry[1]. The three basic elements are-

(i) Pre-processor
(ii) Solver and
(iii) Post-Processor[1]

2.1 MESHING AND PRE-PROCESSING

The pre-processing of the CFD process consists of the input of a flow problem by means of user-friendly programs or software and the successive transformation of this input into a form is made appropriate to use by the solver. The pre-processor is the link between the user and the solver. The user activity at the pre-processing stage of the CFD process involves the following[1]:

1) Explanation of Geometry or region of Interest: This process involves several computer aided design (CAD) software like CATIA, Solidworks, Pro-E and much more[1]

2) Grid Generation or Meshing: Since the CFD process is a numerical approximation method using finite volume method, the given domain or region of interest needs to be divided into several structured elements. All the elements or cells are connected to each other through nodes to form the required region of flow[1].

3) Description of Fluid property: Every fluid domain or Face has its own distinct property. The properties of the fluid used in the CFD domain or region of interest are defined at this stage of the CFD Process. Usually the CFD code software has this facility[1].

4) Boundary Conditions: Every different setup of the CFD domain needs to have an initialization, which is satisfied by the boundary conditions input. The CFD code usually has this facility to define the boundary conditions of the CFD problem, where each cells at specific boundary are given finite values[1].

2.2 NUMERICAL SOLVER

The numerical solver is the key elements of the CFD process and covers the major part of the CFD process. The finite volume method is the most suitable method for the CFD process. As the name implies, finite volume method is the numerical algorithm calculation process relating the use of finite volume cells. The steps occupied in this solving process are usually carried out in the following sequence[1]:

1. Formal integration of the governing equations of fluid flow over all the control volumes or finite volumes of the solution domain.
2. The conversion of the integral forms of the equations into a system of algebraic equations.
3. Calculations of the algebraic equations by an iterative method[1].

2.3 POST PROCESSOR

The post processor is the last phase of the CFD process which involves data visualization and results analysis of the CFD process. This phase uses the versatile data visualization tools of the CFD solver to observe the following results of the simulation[1]:

1. Domain geometry and Grid show
2. Vector plots
3. Line and shaded contour plots
4. 2D and 3D Face plots
5. Particle tracking
6. XY plots and graphs of results[1].

3. Literature Review

A concise appraisal of literature has been provided in the following areas: (a) Aerodynamic Drag (b) Add-on devices (c) Drag reduction using devices.

3.1 Aerodynamic Drag :

Currently we see price of fuel increases enormously due to scarcity of energy resources as a result of which there is a chance of doping of fuel with some needless elements, which influence green house gas emission from vehicle. In order to increase vehicle efficiency there is much stress over automobile designers to improve vehicle design, performance by optimizing vehicle shape more aerodynamically. Aerodynamic drag is one of the main obstacles to speed up a vehicle when it moves in the air. The aerodynamic drags of a road vehicle is responsible for a large part of the vehicle's fuel consumption and contribute up to 50% of the total vehicle fuel consumption at highway speeds.

When the vehicle is moving at an undistributed velocity, the viscous effects in the fluid are restricted to a thin layer called boundary layer. Outside the boundary layer is the inviscid flow. . This fluid flow imposes pressure force on the boundary layer[1].

When the air reaches the rear part of the vehicle, the fluid gets detached. Within the boundary layer, the movement of the fluid is totally governed by the viscous effects of the fluid. The boundary does not exist for the Reynolds Number which is lower than 104. The Reynolds number is dependent on the characteristic length of the vehicle, the kinematic viscosity and the speed of the vehicle. Apparently, the fluid moving around the vehicle is dependent on the shape of the vehicle and the Reynolds number. There is another important phenomenon which affects the flow of the car and the performance of the vehicle.

This phenomenon is commonly known as 'Wake' of the vehicle. When the air moving over the vehicle is separated at the rear end, it leaves a large low pressure turbulent region behind the vehicle known as the wake. This wake contributes to the formation of pressure drag, which is eventually reduces the vehicle performance[1]

FACTORS CONTRIBUTING TO FLOW FIELD AROUND VEHICLE

The major factors which affect the flow field around the vehicle are the boundary layers, separation of flow field, friction drag and lastly the pressure drag[1].

BOUNDARY LAYER: The Aerodynamics boundary layer was first defined by the Aerodynamic engineer 'Ludwig Prandtl' in the conference at Germany. This allows aerodynamicists to simplify the equations of fluid flow by dividing the flow field into two areas: one inside the boundary layer and the one outside the boundary layer. In this boundary layer around the vehicle, the viscosity is dominant and it plays a major role in drag of the vehicle. The viscosity is neglected in the fluid regions outside this boundary layer since it does not have major effect on the solution. In the design of the body shape, the boundary layer is given high attention to reduce drag. There are two reasons why designers consider the boundary layer as a major factor in aerodynamic drag. The first is that the boundary layer adds to the effective thickness of the body, through the displacement thickness, hence increasing the pressure drag. The second reason is that the shear forces at the Face of the vehicle causes skin friction drag[1].

SEPARATION: During the flow over the Face of the

vehicle, there is a point when the change in velocity comes to stall and the fluid starts flowing in reverse direction. This phenomenon is called 'Separation' of the fluid flow. This is usually occurred at the rear part of the vehicle. This separation is highly dependent on the pressure distribution which is imposed by the outer layer of the flow. This phenomenon is the major factor to be considered while studying the wake of the vehicle[1].

FRICTION DRAG: Each wall Face or material has a different friction which resists the flow of fluids. Due to molecular friction, a stress acts on every Face of the vehicle. The combination of the equivalent force component in the free stream path leads to a friction drag. If the separation does not take place, then friction drag is one of the main reasons to cause overall drag[1]

PRESSURE DRAG: The blunt bodies like large size vehicle show different drag characteristics. On the rear part of such vehicles, there is an extremely steep pressure gradient which leads to the separation of the flow separation in viscous flow. The front part of the flow field shows high pressure value, whereas on the rear part flow separates leading to a high suction in the area. As we combine the force component created by such high change in pressure, the resultant is called as 'Pressure Drag'. This factor is affected by the height of the vehicle as well as the separation of the flow field[1]

Force on vehicle:

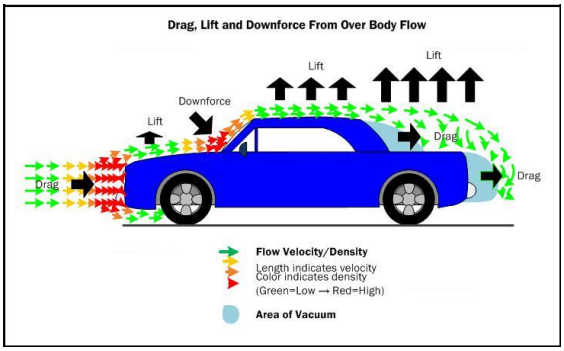

Fig-1: Drag& lift force

Lift force: The vertical force acting on the body indicated by the letter "L" is known as Lift force. This force causes the vehicle to get lifted in air as applied in the positive direction, whereas it can result in excessive wheel down force if it is applied in negative direction. The formula usually used to define this force is written as:

$$L = \tfrac{1}{2}\rho V^2 C_L A \quad \text{----------(1)}$$

Where
L= lift force
CL= Lift coefficient
A= Frontal area of the vehicle

Drag force: Aerodynamic drag force is the force acting on the vehicle body resisting its forward motion. This force is an important force to be considered while designing the external body of the vehicle, since it covers about 65% of the total force acting on the complete body. The Aerodynamic drag force is calculated by the following formula:

$$D = \tfrac{1}{2}\rho V^2 C_D A \text{---------(2)}$$

Where
CD= Drag coefficient

Researches carried out by a number of researchers with regard to control flow separation by variation of external vehicle geometry attaching spoilers, VGs, diffuser, tail-plate, guide vanes etc. Addition of add-on devices considerably improves aerodynamic efficiency of the passenger car. Hence, the drag force can be reduced by using add-on devices on vehicle and fuel economy, stability of a passenger car can be improved[1].

3.2Drag reduction attaching ADD-ON Devices:

Attaching spoiler

The spoiler is used as a device to diminish inauspicious air movement around the vehicle and can be divided into the front spoilers and the rear spoilers. A front spoiler, attached with the bumper, is mainly used to direct air flow away from the tires to the under body. A rear spoiler is usually installed upon the trunk lid of a passenger vehicle. The added spoiler can diffuse the airflow passing a vehicle, which minimizes the turbulence at the rear of the vehicle, adds more downward pressure to the back end and reduces lift acted on the rear trunk [3]

Attaching Diffuser

A diffuser, in an automotive framework, is an arc shaped section of the car underbody. The diffuser improves the car's aerodynamic properties by enhancing the transition between the high-velocity airflow underneath the car and the much slower free stream airflow of the ambient atmosphere. It works by providing a space for the underbody airflow to slow down and spread out so that it does not cause excessive flow separation and drag, by providing a degree of wake infill or more accurately, pressure recovery[3]

Fig -2: Diffuser

Attaching VGs

One of the other method to diminish drag force in car by

means of vortex generators (VGs) at the outer end Face of roof of car. The main purpose of vortex generator is to holdup the air separation. They are small and fit inside the boundary layer, shaped like triangular fins and are especially effective in speeds in excess of 100 kmph[3]

Fig- 3:. Vortex generators

Attaching Tail-plate

Ram Bansal numerically investigated the use of tail- plates as a drag reducing device for ground vehicle, used baseline prototype of passenger car with
and without tail-plates then simulated in CFD.

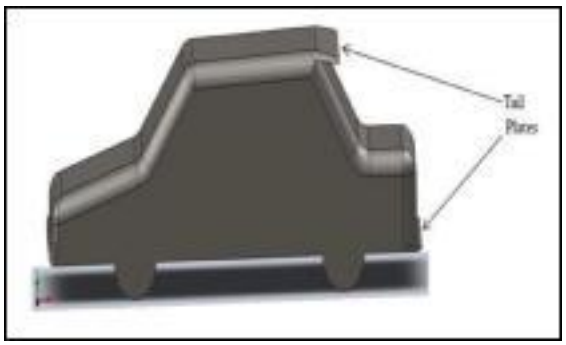

Fig- 4: Car with tail plate[3]

After simulation found that in case of tail plates are applied on the rear bumper and rear side of roof of the base line car respectively with inclination angle 120. The coefficient of drag is 0.3376 and the coefficient of lift is 0.1926. The percentage reduction in drag coefficient in comparison of base line car is 3.87% and in coefficient of lift is 16.62%[3]

4.Outcome from literature Review

The following are the concluding remarks drawn from the reviewed literature:

- Separation zone occurs at the rear and it is in this area that the maximum potential for drag reduction is possible.
- Controlling the rear wake would lead to delay in the separation of the boundary layer which could be done by using add- on devices.
- Drag reduction methods on a car have so far reached saturation and therefore passive methods such as (add – on devices) shows a promising ability to reducing drag without making major changes to the critical body profile of a Sedan car.
- CFD is most popular tool for vehicle aerodynamic analysis as it is cost effective, more informative and faster than wind tunnel experiments.
- Among the Sedan cars and the square back car suffers the most from high amounts of base pressure drag because of separation of boundary layer.
- The aerodynamic drag of a road vehicle is responsible for a large part of the vehicle's fuel consumption and contributes up to 50% of the total vehicle fuel consumption at highway speeds. Reducing the aerodynamic drag offers an inexpensive solution to improve fuel efficiency.
- Conventional passive control techniques, consisting in modifying the shape of the vehicle or attaching add-on devices to reduce the aerodynamic drag, appears as the easiest to implement but unfortunately it only dedicated for particular application. Due to wide range of applications active flow control is preferable. However both methods proved to be able to reduce aerodynamic drag of vehicle thus have potential for fuel economy.
- A large contribution to the aerodynamic drag of a vehicle arises from the failure to fully recover pressure in the wake region, especially on square back configurations. A degree of base pressure recovery can be achieved through casual shape optimisation, but the freedom of an automotive aerodynamicist to implement significant shape changes is limited by a variety of additional factors such styling, ergonomics and loading capacity.

- The review provides information on the methods that could be possibly used to improve fuel efficiency and as guidance for aerodynamic design.
- The relative effectiveness of flow control methods (between active methods) or (between passive methods) is not known as the percentage of drag reduction was compared with base prototype of vehicle as it is different between the experiments.
- The selection of mathematic prototype of flow, Reynolds number, vehicle prototype, design parameters, forcing parameters need for further investigation as it influences the result of aerodynamic drag.

5.Methodology & various steps

In this work, first of all a prototype of the passenger car is prepared in the CATIA software and this prototype is import into the ANSYS FLUENT to do the simulation of the coefficient of drag and coefficient of lift in the wind tunnel which is generated in the design module of the ANSYS FLUENT. After this the meshing is generated on the face of the passenger car.

Aerodynamic assessment of air flow over an object can be performed using analytical method or CFD approach. On one hand, analytical method of solving air flow over an object can be done only for simple flows over simple geometries like laminar flow over a flat plate. If air flow gets complex as in flows over a bluff body, the flow becomes turbulent and it is impossible to solve Navier-Stokes and continuity equations analytically. On the other hand, obtaining direct numerical solution of Navier-stoke equation is not yet achievable even with modern day computers. In order to come up with reasonable solution, a time averaged Navier-Stokes equation is being used (Reynolds Averaged Navier-Stokes Equations – RANS equations) together with turbulent prototypes to resolve the issue involving Reynolds Stress resulting from the time averaging process.

In present work the k -e turbulence prototype with non-equilibrium wall function is selected to analyze the flow over the passenger car prototype. This k-e turbulence prototype is very robust, having reasonable computational turnaround time, and widely used by the auto industry[4]

Steps of Analysis:

- Select the prototype of vehicle ahead which add on devices are to be used.
- Formation of Baseline prototype : Designing of prototype in CATIA with proper aspect& parameters
- Baseline passenger car CFD method & setup: Apply the boundary conditions.
- Generate the wind tunnel for simulation.
- Simulation& testing of baseline passenger car for drag coefficient & lift coefficient
- Simulation & testing of baseline passenger car with spoiler, tail -plate, VGs, splines.
- Impact of add-on devices on fuel economy[4]

6. BASELINE PROTOTYPE

The base line prototype of passenger car is designed in CATIA. Then after, this prototype has been analyzed for drag coefficient and forces under the HYPERMESH (FULENT) module and values of drag coefficient, lift coefficient.

1. Summary

This report summarize the outcome of an exterior aerodynamic CFD analysis performed by Altair's Virtual Wind Tunnel, leveraging AcuSolve's CFD technology. The first section provides a short overview of the run and its results.

Table -1: Problem statement

Simulation form	"transient"
Element count	532321
CPU period	0.029h
Inflow velocity	30 m/s
Drag coefficient,C_d	0.603
Lift coefficient, C_l	0.250

2. Aspects

This sections contains geometric aspects related to the wind tunnel and the body.

Table -2: Geometric aspect

Wind tunnel, bound box	[0.000, 7.000], [-2.000, 2.000], [0.000, 3.000]
Body, bound box	[1.661, 4.140], [-0.540, 0.540], [0.039, 1.224]
Wind tunnel aspect	8.000 m x 5.000 m x 4.000 m.
Body aspect	2.478 m x 1.080 m x 1.185 m.
Frontal ref. area, A	1.0363 m^2
Blockage ratio %	8.63583333333
Distance inflow – body	1.661 m

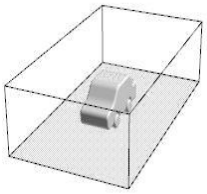

Fig -5: Virtual wind tunnel

3. Mesh

This section contains mesh figures and screen shots of several cutting planes through the mesh

Table 3: Mesh figures

Number of nodes	99025
Number of elements	532321
Number of refinement zones	0

Table- 4:Cutting planes through mesh

Figure 6	Equilibrium plane
Figure 7	Traverse section

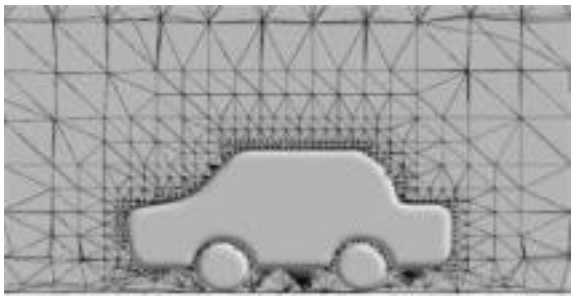

Fig -6: Flow Direction Meshing

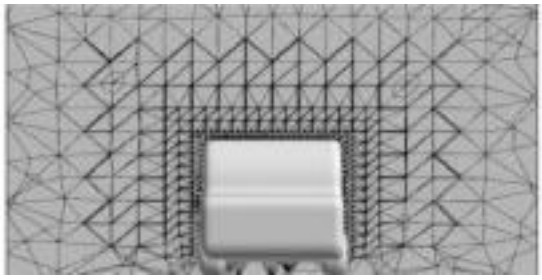

Fig -7: Traverse Direction Meshing

D. Boundary Conditions and Solution Strategy

In this section the boundary conditions and the setup for the CFD run are listed

Table -5: Boundary conditions

Inflow velocity	30 m/s
Outflow	Pressure outlet
Slip Walls	Top, right, left faces of wind tunnel
No-slip Walls	wind tunnel ground, body, wheels, heat-exchange

Table- 6: Solution Strategy

Simulation form	"transient"
Number of time steps	5
Time rise	0.2
Physical time	1.000
Turbulence prototype	Detached Eddy Simulation
Moving ground	True
Rotating wheels	True

5. Results

In this section the results of the CFD run are reported. Table7 gives an impression of the different result types[5]

Table -7: Results

Table 8	Drag & lift coefficient of car
Table 9	Drag area of car
Figure 8,9,10	Pressure contours on body, equilibrium and Traverse section plane
Figure11	Pressure coefficient on body Face
Figure 12,13	Velocity contours on Equilibrium and horizontal cut plane
Figure 14,15	Front & side view of streamlines around body
Figure 16,17,18	Body Face y+ views

Table- 8: Coefficient

Face	Drag Coefficient	Lift Coefficient
Car	0.603	0.250

Table- 9: Drag Areas

Face	Drag Area
Car	0.62573

To compute the above aerodynamic coefficients, the following equations are used

Drag coefficient, C_d = $\frac{2\,Fx}{\rho\, v^2\, A}$

Lift coefficient, C_l = $\frac{2\,F_y}{\rho\, v^2\, A}$

Fx; Fy; forces are acting on the body in x, y and z directions, respectively

ρ is density of air (1.225 kg/m3)
v is free stream velocity

A is frontal projected area of the object[5]

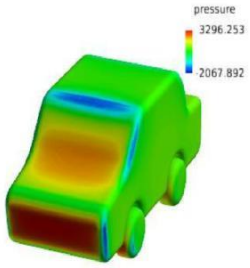

Fig -8: Body Face Pressure Contour

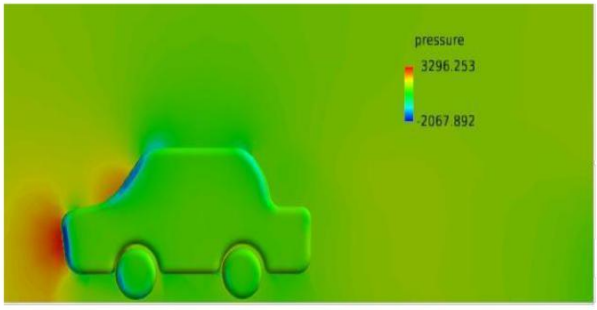

Fig -9: Mean Plane Pressure Contour

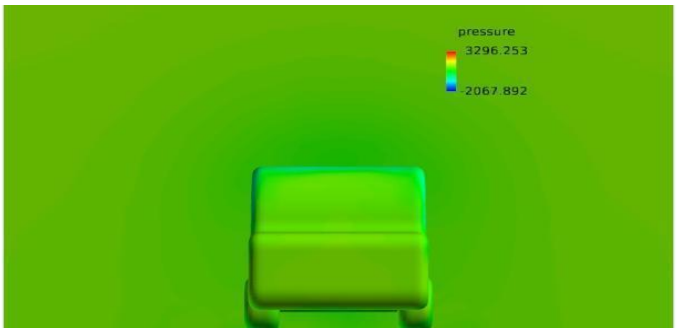

Fig -10: Traverse Plane Pressure Contour

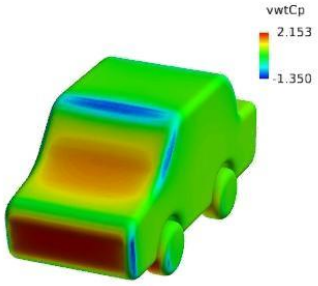

Fig- 11: Body Face Pressure Coefficient

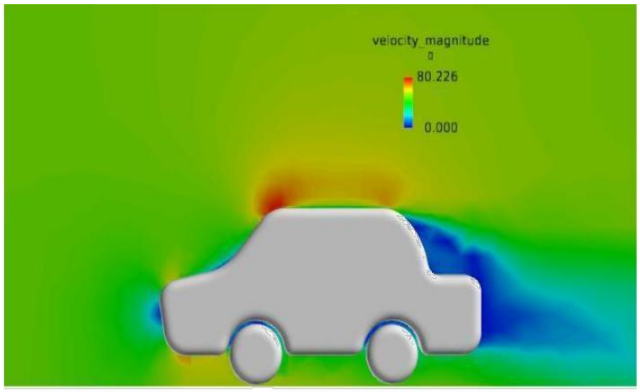

Fig -12: Mean Plane Velocity Contours

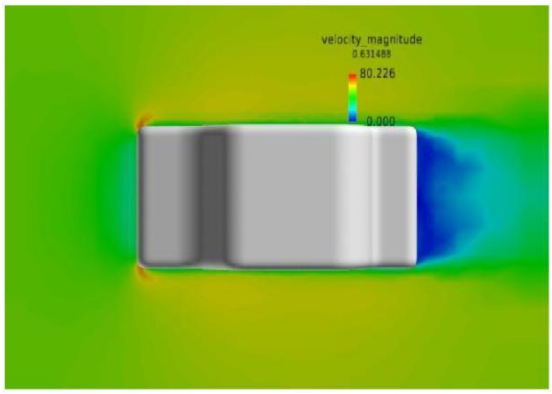

Fig -13: Traverse Plane Velocity Contours

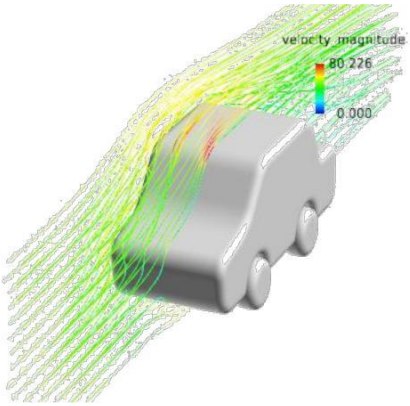

Fig- 14: Front view of streamlines

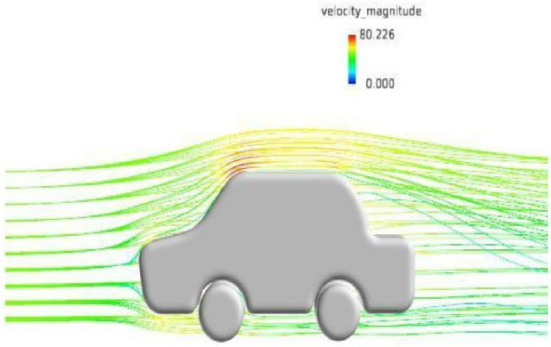

Fig -15: Side view of streamlines

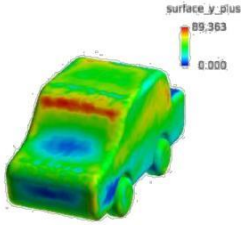

Fig -16: Body Face y + front view

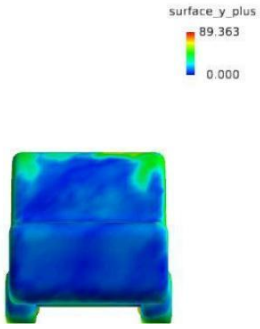

Fig -17: Body Face y + rear view

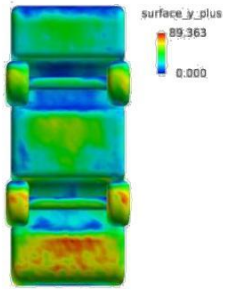

Fig -18: Body Face y + bottom view

7. Passenger car with Splines

The prototype of passenger car is designed in CATIA. Then after, this prototype has been analyzed for drag coefficient and forces under the HYPERMESH (FULENT) module and values of drag coefficient, lift coefficient.

1.Summary

This result summarizes the outcome of an exterior aerodynamic CFD analysis performed by Altair's Virtual Wind Tunnel, leveraging AcuSolve's CFD technology. The first section provides a short overview of the run and its result.

Table -10: Problem statement

Simulation form	"transient"
Element count	1002278
CPU period	0.114 h
Inflow velocity	30 m/s
Drag coefficient, C_d	0.590
Lift coefficient, C_l	0.235

2.Aspects

This sections contains geometric aspects related to the wind tunnel and the body.

Table- 11: Geometric Aspect

Wind tunnel, bound box	[0.000, 7.000], [-2.000, 2.000], [0.000, 3.000]
Body, bound box	[2.607, 5.086], [-0.540, 0.540], [0.051, 1.247]
Wind tunnel aspect	8.000 m x 5.000 m x 4.000 m
Body aspect	2.478 m x 1.080 m x 1.196 m.
Frontal ref. area, A	1.0462 m^2
Blockage ratio %	8.71833333333
Distance inflow - body	2.607 m

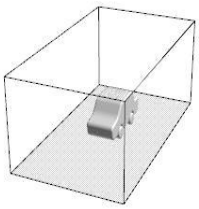

Fig -19: Virtual wind tunnel

3.Mesh

This section contains mesh figures and screen shots of several cutting planes through the mesh.

Table-12. Mesh figures

Number of nodes	181555
Number of elements	1002278
Number of refinement zones	0

Table -13: Cutting planes through Mesh

Figure 20	Equilibrium plane
Figure 21	Traverse section

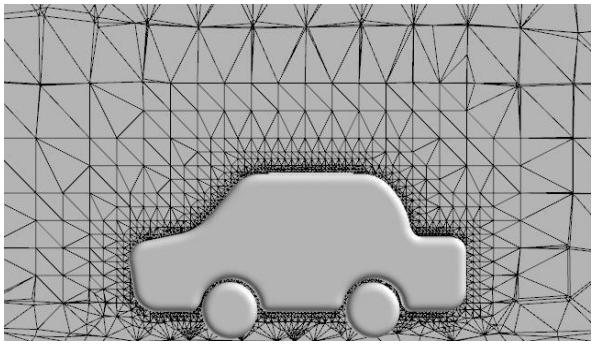

Fig- 20: Flow Direction Meshing

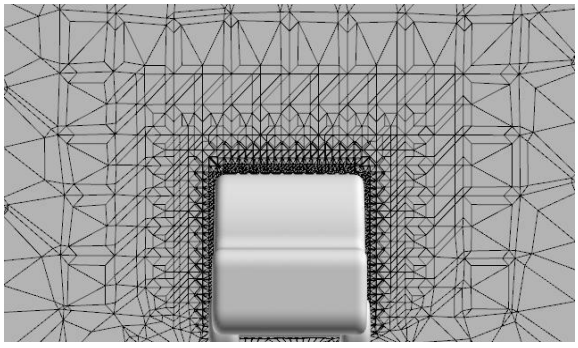

Fig- 21: Traverse direction Meshing

4. Boundary condition and solution strategy

In this section the boundary conditions and the setup for the CFD run are listed.

Table -14: Boundary conditions

Inflow velocity	30 m/s
Out flow	Pressure outlet
Slip Walls	Top, right, left faces of wind tunnel
No-slip Walls	wind tunnel ground, body, wheels, heat-exchange

Table -15: Solution strategy

Simulation form	"transient"
Number of time steps	10
Time rise	0.2
Physical time	2.000
Turbulence prototype	Detached Eddy Simulation
Moving ground	True
Rotating wheels	True

5. Results

In this section the results of the CFD run are reported. Table7 gives an impression of the different result types[5]

Table -16: Results

Table 17	Drag & lift coefficient of car
Table 18	Drag area of car
Figure 22 23,24	Pressure contours on body, Equilibrium and Traverse section plane
Figure 25	Pressure coefficient on body Face
Figure 26,27	Velocity contours on Equilibrium and horizontal cut plane
Figure 28,29	Front view of streamlines around body
Figure 30,31,32	Body Face y+ views

Table- 17: Coefficients

Face	Drag Coefficient	Lift Coefficient
Car	0.590	0.235

Table- 18: Drag areas

Face	Drag area
Car	0.66564

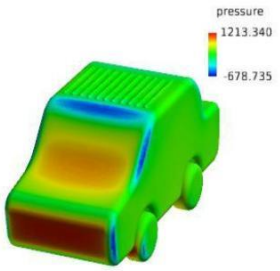

Fig -22: Body Face pressure contour

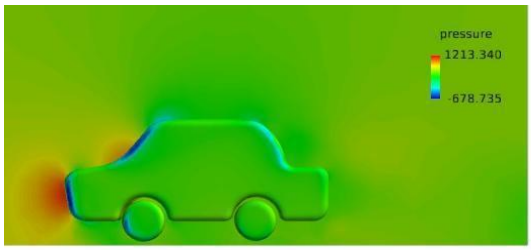

Fig -23. Mean plane pressure contour

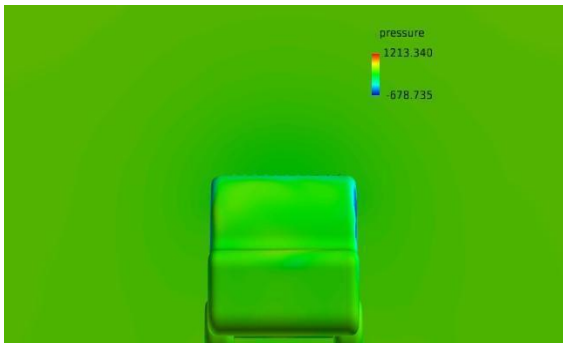

Fig -24: Traverse plane pressure contour

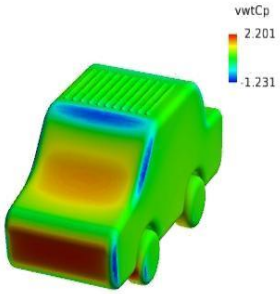

Fig -25: Body Face pressure coefficient

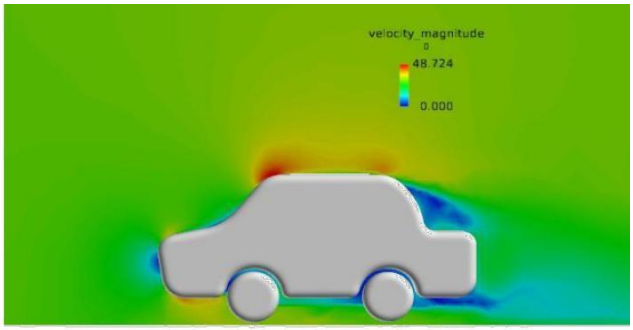

Fig -26: Mean plane velocity contour

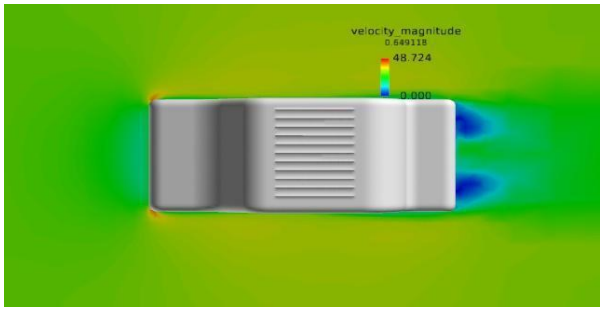

Fig- 27: Traverse plane velocity contour

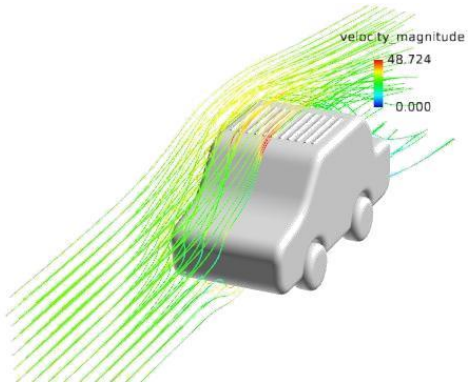

Fig -28: Front view of streamlines

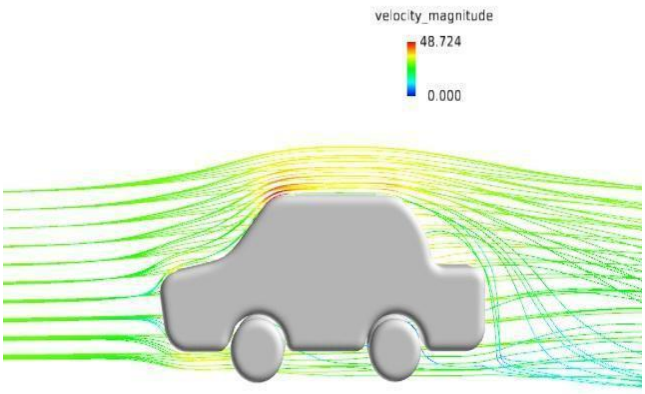

Fig- 29: Side view of streamlines

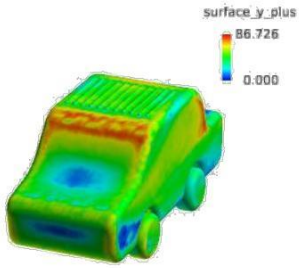

Fig -30: Body Face y + front view

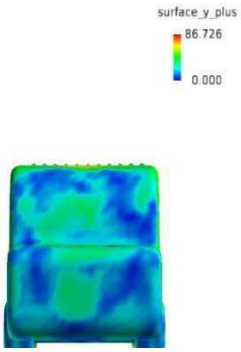

Fig -31: Body Face y + rear view

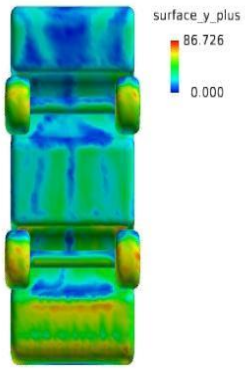

Fig -32: Body Face y + bottom view

8. Passenger car with spoiler

The prototype of passenger car is designed in CATIA. Then after, this prototype has been analyzed for drag coefficient and forces under the HYPERMESH (FULENT) module and values of drag coefficient, lift coefficient

1.Summary
This report summarizes the outcome of an exterior aerodynamic CFD analysis performed by Altair's Virtual Wind Tunnel, leveraging AcuSolve's CFD technology. The first section provides a short overview of the run and its results.

Table -19: Problem statement

Simulation form	"transient"
Element count	632747
CPU period	0.042 h
Inflow velocity	30 m/s
Drag coefficient, Cd	0.570
Lift coefficient, Cl	0.230

2.Aspects
This sections contains geometric aspects related to the wind tunnel and the body.

Table- 20: Geometric aspects

Wind tunnel, bound box	[0.000, 7.000], [-2.000, 2.000], [0.000, 3.000]
Body, bound box	[1.295, 3.673], [-0.423, 0.677], [0.073, 1.098]
Wind tunnel aspect	8.000 m x 5.000 m x 4.000 m.
Body aspect	2.378 m x 1.100 m x 1.025 m.
Frontal ref. area, A	0.91344 m^2
Blockage ratio %	7.612
Distance inflow - body	1.295 m

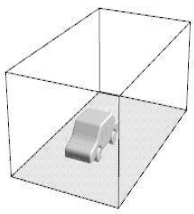

Fig -33: Virtual wind tunnel

3.Mesh
This section contains mesh figures and screen shots of several cutting planes through the mesh.

Table- 21: Mesh figures

Number of nodes	115687
Number of elements	632747
Number of refinement zones	0

Table- 22: cutting planes through Section

Figure 34	Equilibrium plane
Figure 35	Traverse section

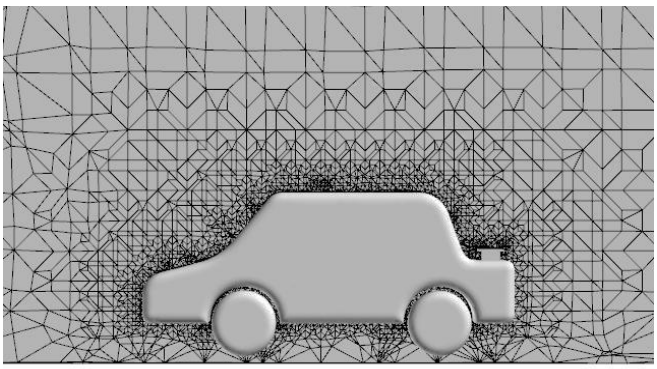

Fig- 34: Flow Direction Meshing

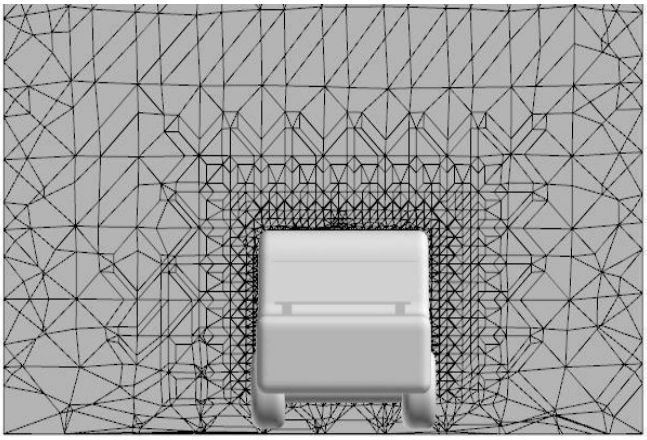

Fig -35: Traverse Direction Meshing

4. Boundary condition & solution strategy

In this section the boundary conditions and the setup for the CFD run are listed.

Table -23: Boundary condition

Inflow velocity	30 m/s
Outflow	Pressure outlet
Slip Walls	Top, right, left faces of wind tunnel
No-slip Walls	wind tunnel ground, body, wheels, heat-exchange

Table -24: Solution strategy

Simulation form	"transient"
Number of time steps	5
Time rise	0.4
Physical time	2.000
Turbulence prototype	Detached Eddy Simulation
Moving ground	True
Rotating wheels	True

5.Results

In this section the results of the CFD run are reported. Table 25 gives an impression of the different result types.

Table -25: Results

Table 26	Drag & lift coefficient of car
Table 27	Drag area of car
Figure 36,37,38	Pressure contours on body, Equilibrium and Traverse section plane
Figure 39	Pressure coefficient on body Face
Figure 40,41	Velocity contours on Equilibrium and horizontal cut plane
Figure 42,43	Front & side view of streamlines around body
Figure 44,45,46	Body Face y+ views

Table -26: Coefficient

Face	Drag Coefficient	Lift Coefficient
Car	0.570	0.230

Table- 27: Drag area

Face	Drag Area
Car	0.61771

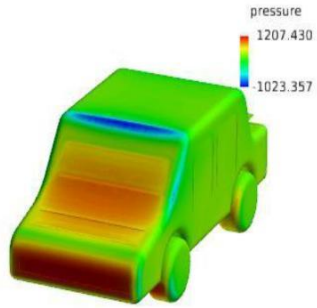

Fig- 36. Body Face pressure contour

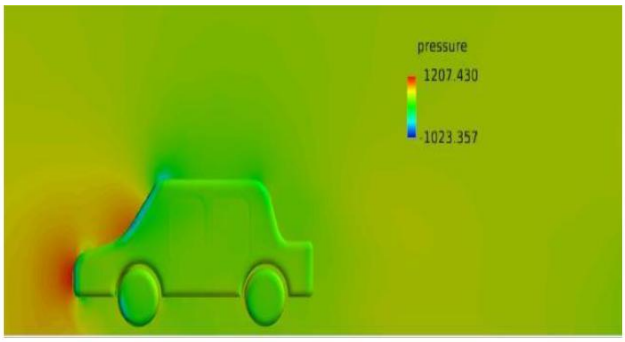

Fig -37. Mean plane pressure contour

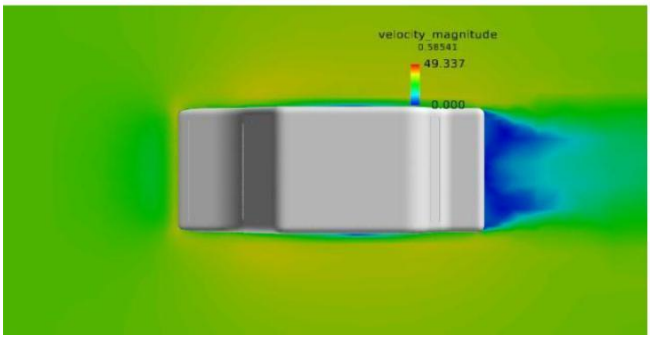

Fig -38 Traverse plane pressure contour

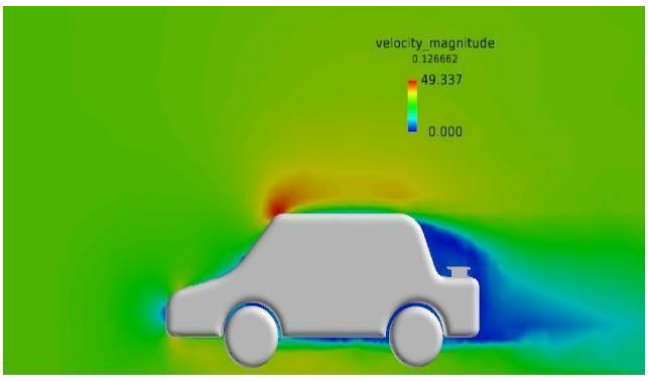

Fig -39. Mean plane velocity contour

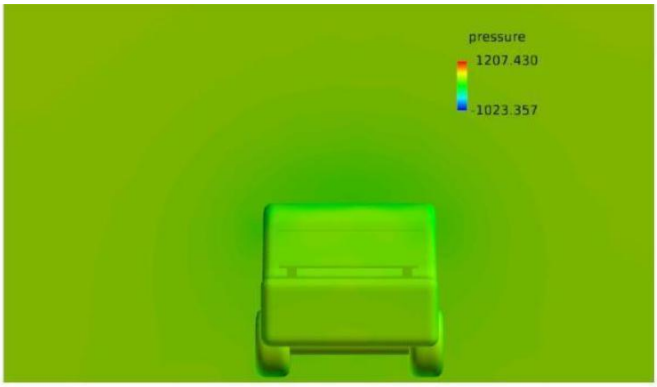

Fig -40. Traverse plane velocity contour

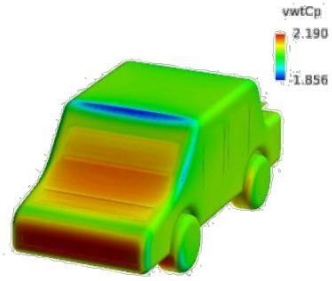

Fig.-41 Body Face pressure coefficient

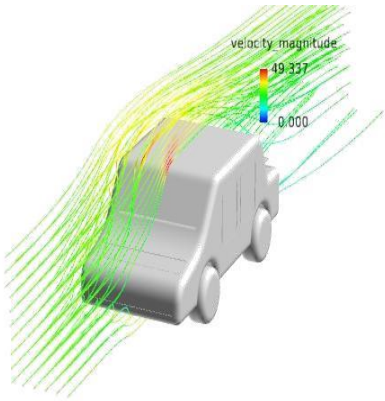

Fig- 42. Front view of streamlines

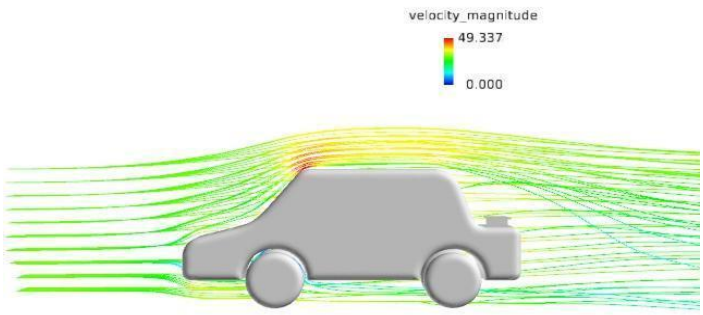

Fig- 43. Side view of streamlines

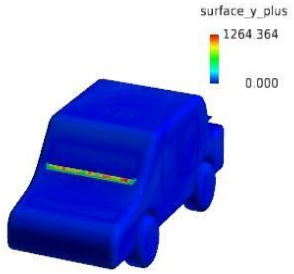

Fig -44. Body Face y + Front view

Fig -45 Body Face y + Rear view

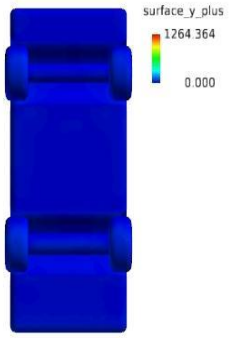

Fig -46. Body Face y + Bottom view

9. Passenger car with Tail- plate

The prototype of passenger car is designed in CATIA. Then after, this prototype has been analyzed for drag coefficient and forces under the HYPERMESH (FULENT) module and values of drag coefficient, lift coefficient[5].

1.Summary

This report summarizes the outcome of an exterior aerodynamic CFD analysis performed by Altair's Virtual Wind Tunnel, leveraging AcuSolve's CFD technology. The first section provides a short overview of the run and its results[5].

Table -28. Problem statement

Simulation form	"transient"
Element count	972857
CPU period	0.046 h
Inflow velocity	30 m/s
Drag coefficient, C_d	0.595
Lift coefficient, C_l	0.240

2.Aspects

This sections contains geometric aspects related to the wind tunnel and the body.

Table -29. Geometric aspects

Wind tunnel, bound box	[0.000, 7.000], [-2.000, 2.000], [0.000, 3.000]
Body, bound box	[1.494, 4.046], [-0.540, 0.540], [0.039, 1.224
Wind tunnel aspect	8.000 m x 5.000 m x 4.000 m
Body aspect	2.552 m x 1.080 m x 1.185 m.
Frontal ref. area, A	1.0363 m^2
Blockage ratio %	8.63583333333
Distance inflow - body	1.494 m

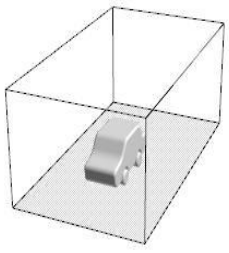

Fig -47: Virtual wind tunnel

3.Mesh

This section contains mesh figures and screen shots of several cutting planes through the mesh.

Table -21. Mesh figures

Number of nodes	115687
Number of elements	632747
Number of refinement zones	0

Table -22. cutting planes through Section

Figure 34	Equilibrium plane
Figure 35	Traverse section

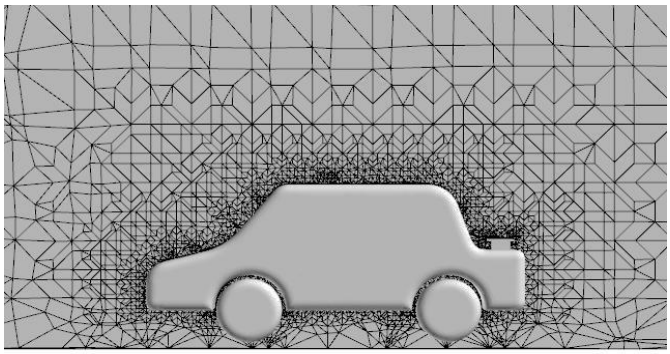

Fig -48. Flow Direction Meshing

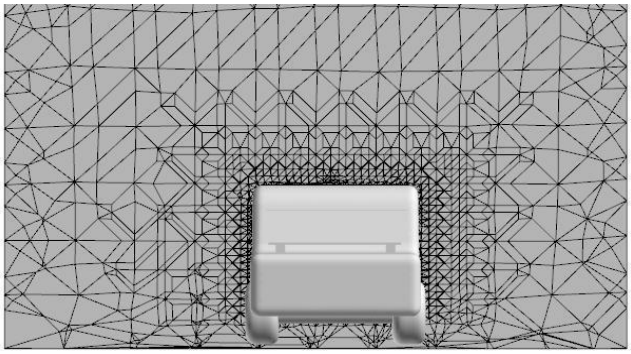

Fig-49. Traverse Direction Meshing

4. Boundary condition & solution strategy

In this section the boundary conditions and the setup for the CFD run are listed.

Table- 23. Boundary condition

Inflow velocity	30 m/s
Outflow	Pressure outlet
Slip Walls	Top, right, left faces of wind tunnel
No-slip Walls	wind tunnel ground, body, wheels, heat-exchange

Table- 24. Solution strategy

Simulation form	"transient"
Number of time steps	5
Time rise	0.4
Physical time	2.000
Turbulence prototype	Detached Eddy Simulation
Moving ground	True
Rotating wheels	True

5.Results

In this section the results of the CFD run are reported. Table 25 gives an impression of the different result types.

Table -25. Results

Table 26	Drag & lift coefficient of car
Table 27	Drag area of car
Figure 50,51,52	Pressure contours on body, Equilibrium and Traverse section plane
Figure 53	Pressure coefficient on body Face
Figure 54,55	Velocity contours on Equilibrium and horizontal cut plane
Figure 56,57	Front & side view of streamlines around body
Figure 58,59,60	Body Face y+ views

Table- 26. Coefficient

Face	Drag Coefficient	Lift Coefficient
Car	0.570	0.230

Table -27. Drag area

Face	Drag Area
Car	0.61771

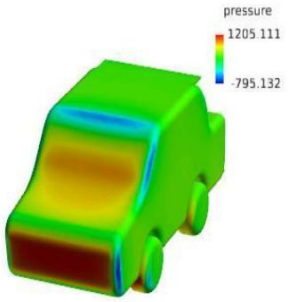

Fig -50: Body Face pressure contour

Fig -51. Mean plane pressure contour

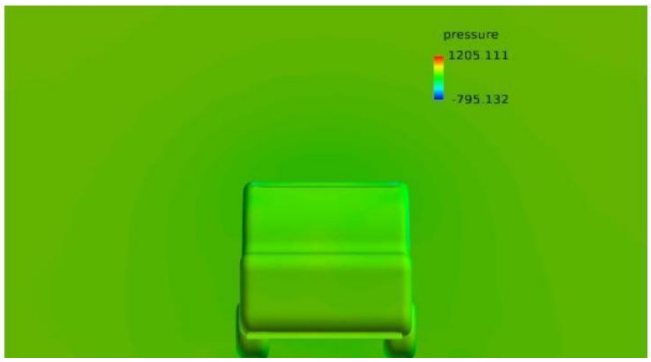

Fig -52 Traverse plane pressure contour

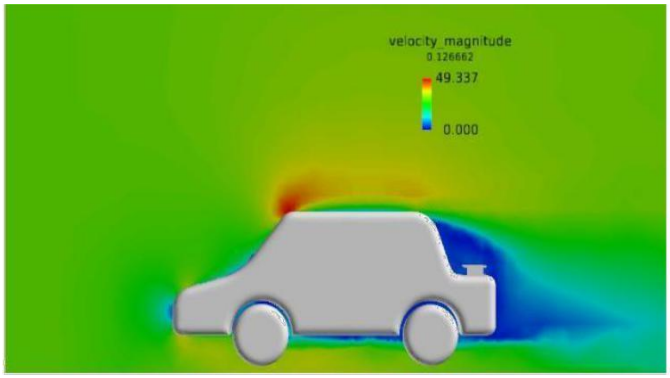

Fig- 53. Mean plane velocity contour

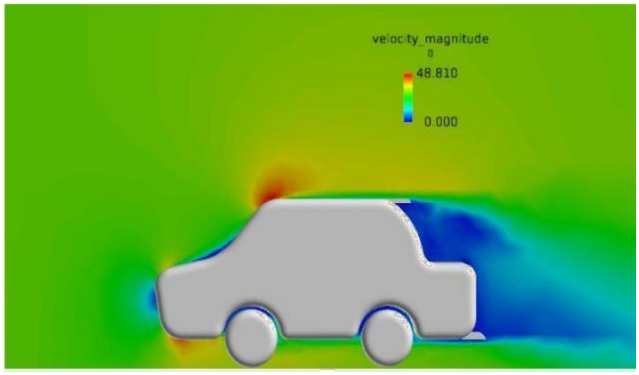

Fig- 54. Traverse plane velocity contour

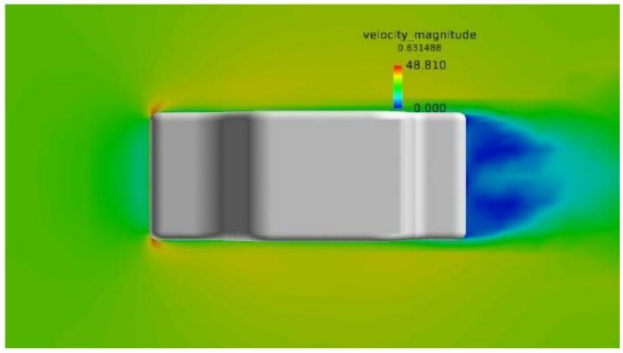

Fig-55 Body Face pressure coefficient

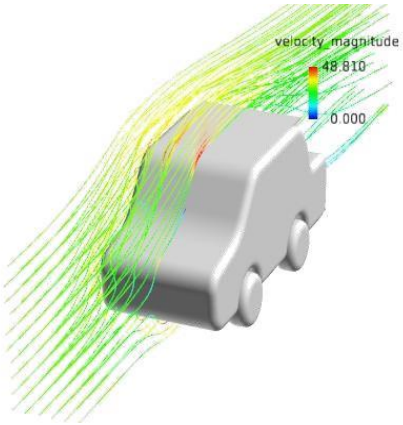

Fig -56. Front view of streamlines

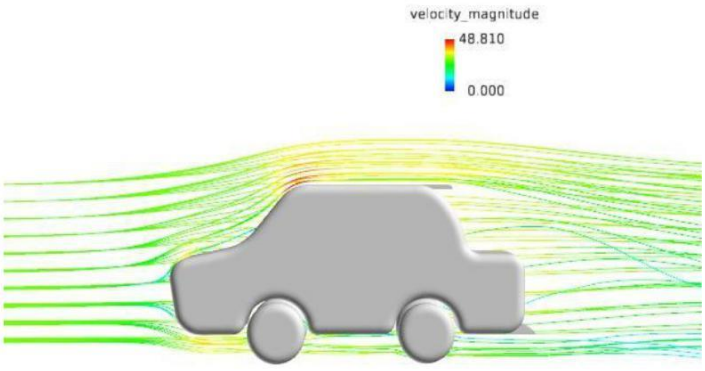

Fig- 57. side view of streamlines

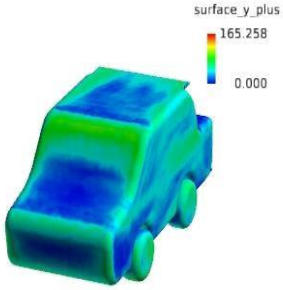

Fig -58. Body Face y + Front view

Fig -59 Body Face y + Rear view

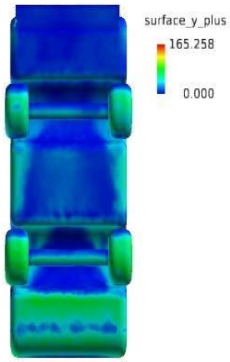

Fig -60. Body Face y + Bottom view

10. Passenger car with VGs

The prototype of passenger car is designed in CATIA. Then after, this prototype has been analyzed for drag coefficient and forces under the HYPERMESH (FULENT) module and values of drag coefficient, lift coefficient.

1.Summary

This report summarizes the outcome of an exterior aerodynamic CFD analysis performed by Altair's Virtual Wind Tunnel, leveraging AcuSolve's CFD technology. The first section provides a short overview of the run and its results].

Table -37. Problem statement

Simulation form	"transient"
Element count	999384
CPU period	0.117 h
Inflow velocity	30 m/s
Drag coefficient, Cd	0.580
Lift coefficient, Cl	0.232

2.Aspects

This sections contains geometric aspects related to the wind tunnel and the body.

Table- 38. Geometric aspects

Wind tunnel, bound box	[0.000, 7.000], [-2.000, 2.000], [0.000, 3.000]
Body, bound box	[2.941, 5.420], [-0.540, 0.540], [0.036, 1.242]
Wind tunnel aspect	8.000 m x 5.000 m x 4.000 m.
Body aspect	2.478 m x 1.080 m x 1.205 m.
Frontal ref. area, A	1.0545 m^2
Blockage ratio %	8.7875
Distance inflow - body	2.941 m

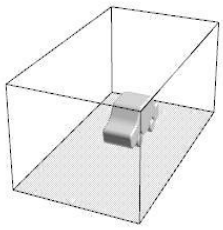

Fig -61. Virtual wind tunnel

3.Mesh

This section contains mesh figures and screen shots of several cutting planes through the mesh.

Table -39. Mesh figures

Number of nodes	181346
Number of elements	999384
Number of refinement element	0

Table -40 Cutting planes through Mesh

Figure 62	Equilibrium planes
Figure 63	Traverse section

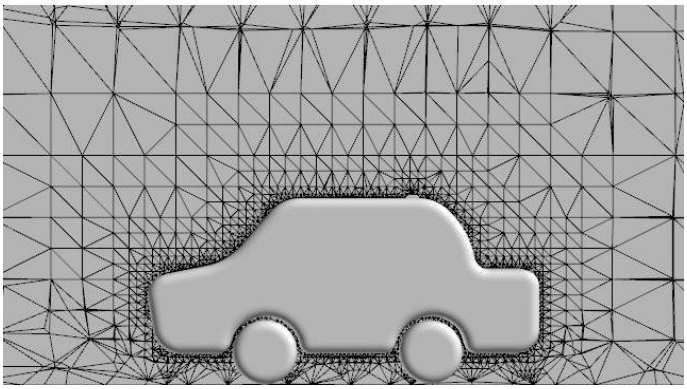

Fig- 62. Flow direction Meshing

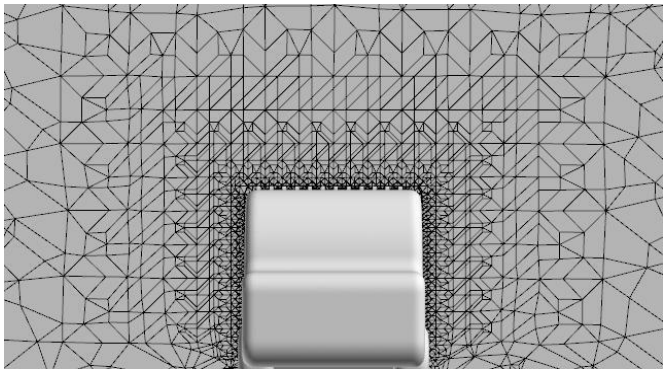

Fig -63. Traverse direction Meshing

4. Boundary condition & solution strategy

In this section the boundary conditions and the setup for the CFD run are listed.

Table -41. Boundary conditions

Inflow velocity	30 m/s
Outflow	Pressure outlet
Slip Walls	Top, right, left faces of wind tunnel
No-slip Walls	wind tunnel ground, body, wheels, heat-exchange

Table- 42. Solution strategy

Simulation form	"transient"
Number of time steps	10
Time rise	0.2
Physical time	2.000
Turbulence prototype	Detached Eddy Simulation
Moving ground	True
Rotating wheels	True

5.Results

In this section the results of the CFD run are reported.
Table 43 gives an impression of the different result types.

Table- 43. Results

Table 44	Drag & lift coefficient of car
Table 45	Drag area of car
Figure 64,65,66	Pressure contours on body, Equilibrium and Traverse section
Figure 67	Pressure coefficient on body Face
Figure 68,69	Velocity contours on Equilibrium and horizontal cut plane
Figure 70,71	Front & side view of streamlines around body
Figure 72,73,74	Body Face y+ views

Table- 44. Coefficients

Face	Drag area
Car	0.68837

Table- 45. Drag areas

Face	Drag coefficients	Lift coefficients
Car	0.580	0.232

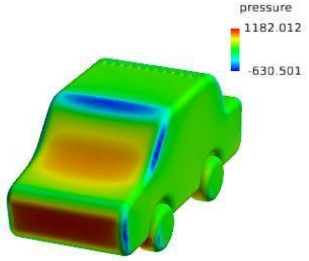

Fig -64. Body Face pressure contour

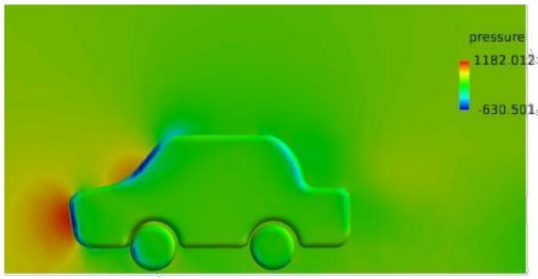

Fig -65. Mean plane pressure contour

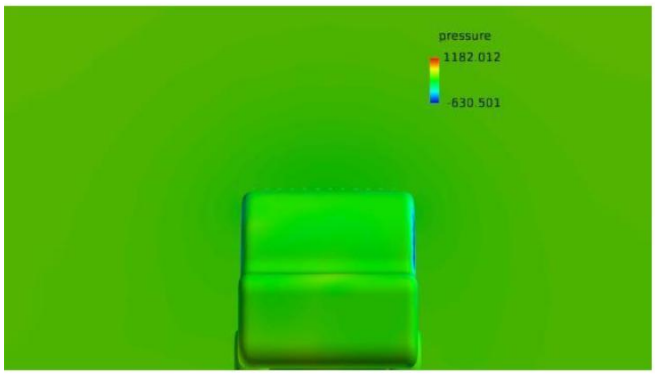

Fig -66. Traverse plane pressure contour

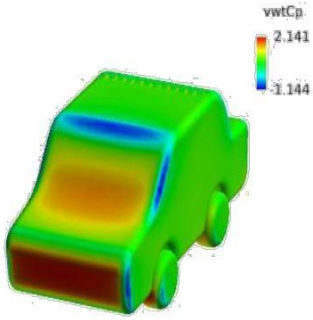

Fig- 67. Body Face pressure coefficient

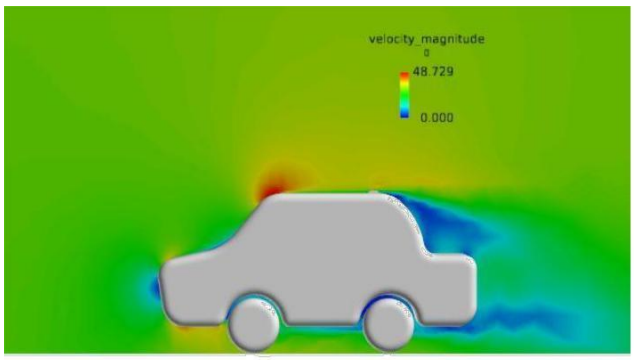

Fig -68. Mean plane velocity contour

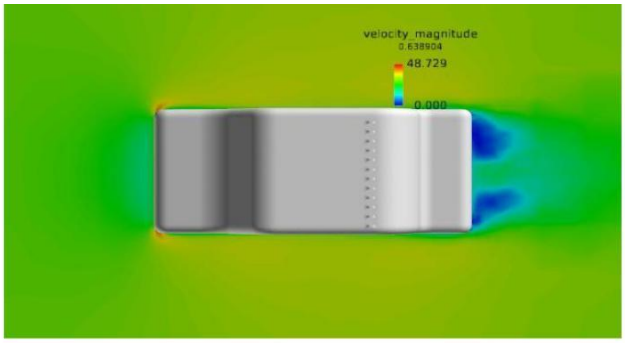

Fig -69. Traverse plane velocity contour

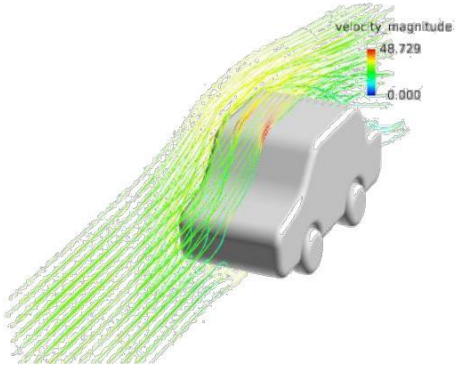

Fig -70. Front view of streamlines

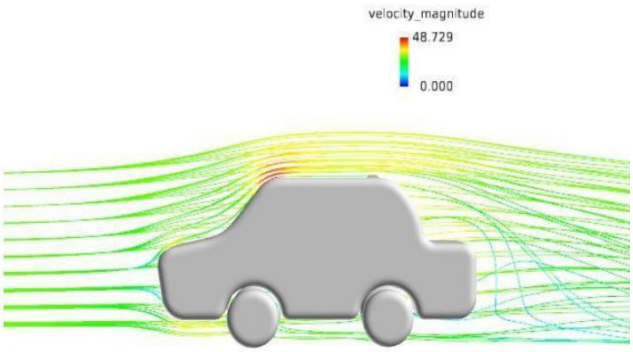

Fig -71. Side view of streamlines

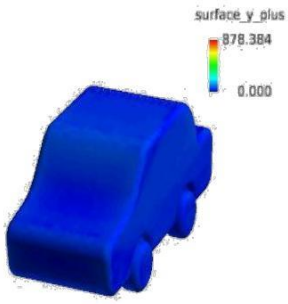

Fig- 72. Body Face y + front view

Fig -73. Body Face y + rear view

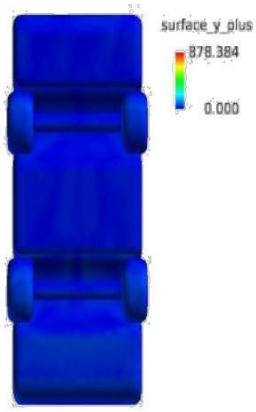

Fig -74. Body Face y + bottom view

11. Passenger car with Spline and Spoiler

The prototype of passenger car is designed in CATIA. Then after, this prototype has been analyzed for drag coefficient and forces under the HYPERMESH (FULENT) module and values of drag coefficient, lift coefficient.

1.Summary

This report summarizes the outcome of an exterior aerodynamic CFD analysis performed by Altair's Virtual Wind Tunnel, leveraging AcuSolve's CFD technology .The first section provides a short overview of the run and its results.

Table- 46. Problem statement

Simulation form	"transient"
Element count	1054672
CPU period	0.050 h
Inflow velocity	30 m/s
Drag coefficient, Cd	0.565
Lift coefficient, Cl	0.225

2. Aspects

This sections contains geometric aspects related to the wind tunnel and the body.

Table - 47. Geometric Aspects

Wind tunnel, bound box	[0.000, 7.000], [-2.000, 2.000], [0.000, 2.000]
Body, bound box	[1.897, 4.376], [-0.540, 0.540], [0.102, 1.298
Wind tunnel aspect	8.000 m x 5.000 m x 4.000 m.
Body aspect	2.478 m x 1.080 m x 1.196 m.
Frontal ref. area, A	1.0462 m^2
Blockage ratio %	13.0775
Distance inflow - body	1.897 m

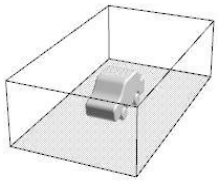

Fig -75. Virtual wind tunnel

3. Mesh

This section contains mesh figures and screen shots of several cutting planes through the mesh.

Table -48. Mesh figures

Number of nodes	190858
Number. of elements	1054672
Number of refinement zones	0

Table- 49. Cutting plane through mesh

Figure 76	Equilibrium plane
Figure 77	Traverse section

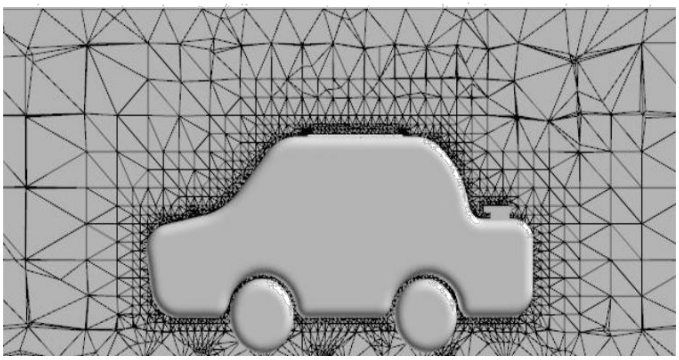

Fig -76. Flow Direction Meshing

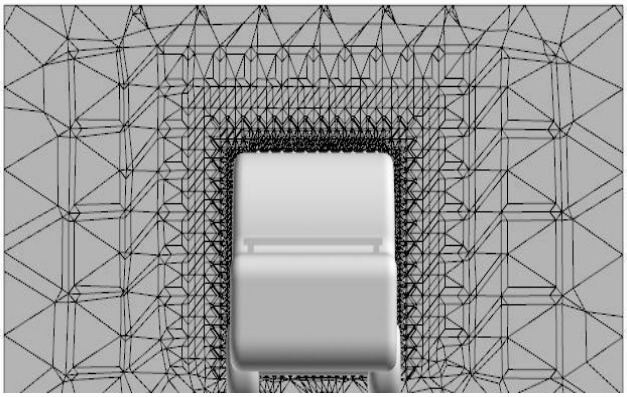

Fig -77. Traverse Direction Meshing

4. Boundary condition & solution strategy

In this section the boundary conditions and the setup for the CFD run are listed.

Table -50. Boundary condition

In flow velocity	30 m/s
Outflow	Pressure outlet
Slip Walls	Top, right, left faces of wind tunnel
No-slip Walls	wind tunnel ground, body, wheels, heat-exchange

Table -51. Solution strategy

Simulation form	"transient"
Number of time steps	4
Time rise	0.5
Physical time	2.000
Turbulence prototype	Detached Eddy Simulation
Moving ground	True
Rotating wheels	True

5. Results

In this section the results of the CFD run are reported. Table 52 gives an impression of the different result types.

Table -52. Results

Table 53	Drag & lift coefficient of car
Table 54	Drag area of car
Figure 78,79,80	Pressure contours on body, Equilibrium and Traverse section plane
Figure 81	Pressure coefficient on body Face
Figure 82,83	Velocity contours on Equilibrium and horizontal cut plane
Figure 84,85	Front & side view of streamlines around body
Figure 86,87,88	Body Face y+ views

Table -53. Drag coefficients

Face	Drag Coefficient	Lift Coefficient
Car	0.565	0.225

Table- 54. Drag area

Face	Drag area
Car	0.53487

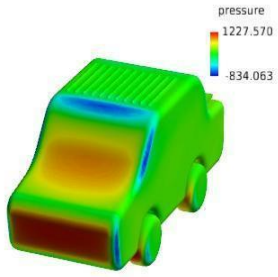

Fig -78. Body Face pressure contour

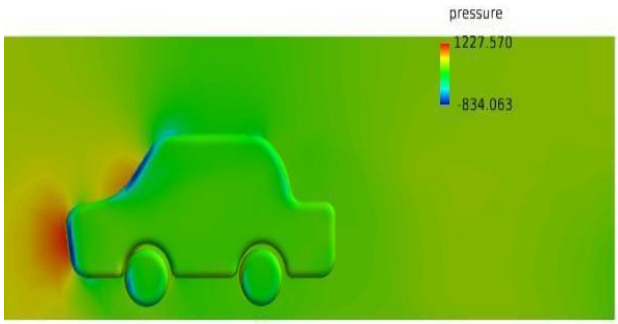

Fig -79. Mean plane pressure contour

Fig -80. Traverse plane pressure contour

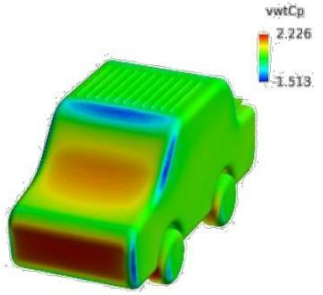

Fig- 81. Body Face pressure coefficient

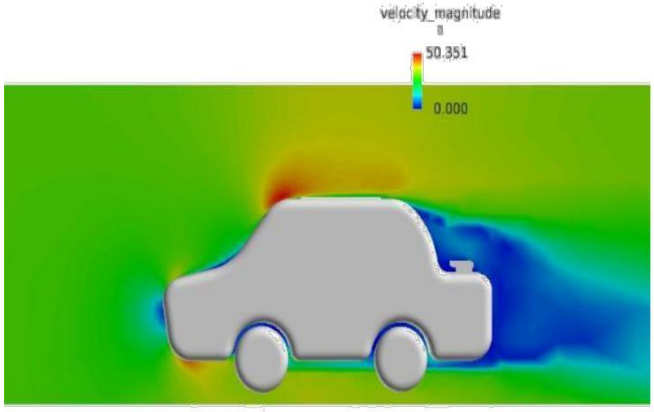

Fig- 82. Mean plane velocity contour

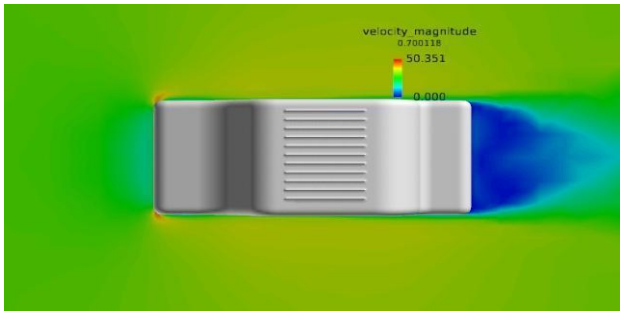

Fig -83. Traverse plane velocity contour

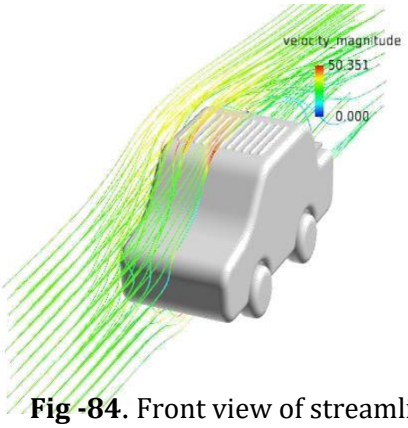

Fig -84. Front view of streamlines

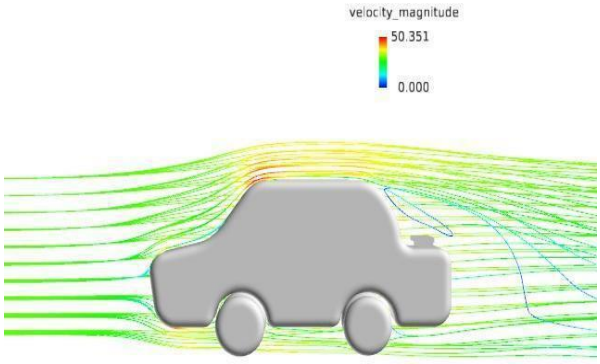

Fig -85. Side view of streamlines

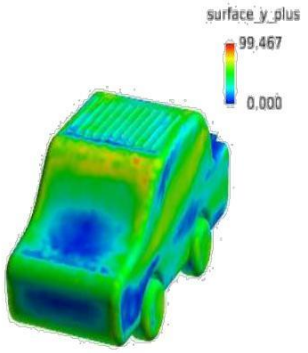

Fig -86. Body Face y + front view

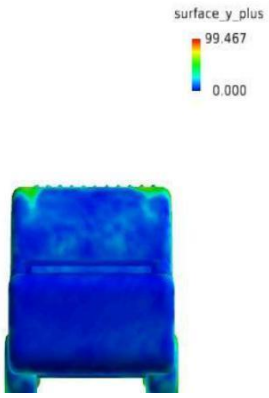

Fig- 87. Body Face y + rear view

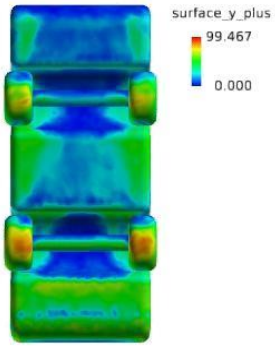

Fig- 88. Body Face y + bottom view

12. Passenger car with VGs and spoiler

The prototype of passenger car is designed in CATIA. Then after, this prototype has been analyzed for drag coefficient and forces under the HYPERMESH (FULENT) module and values of drag coefficient, lift coefficient.

1.Summary
This report summarizes the outcome of an exterior aerodynamic CFD analysis performed by Altair's Virtual Wind Tunnel, leveraging AcuSolve's CFD technology. The first section provides a short impression of the run and its results.

Table -55. problem statement

Simulation form	"transient"
Element count	1038099
CPU period	0.122 h
Inflow velocity	30 m/s
Drag coefficient, Cd	0.550
Lift coefficient, Cl	0.218

2.Aspects
This sections contains geometric aspects related to the wind tunnel and the body.

Table- 56. Geometric aspect

Wind tunnel, bound box	[0.000, 7.000], [-2.000, 2.000], [0.000, 3.000]
Body, bound box	[1.477, 3.956], [-0.540, 0.540], [0.042, 1.263]
Wind tunnel aspect	8.000 m x 5.000 m x 4.000 m.
Body aspect	2.478 m x 1.080 m x 1.221 m.
Frontal ref. area, A	1.0683 m^2
Blockage ratio %	8.9025
Distance inflow - body	1.477 m

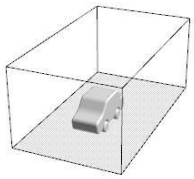

Fig -89 Virtual wind tunnel

3.Mesh
This section contains mesh figures and screen shots of several cutting planes through the mesh.

Table -57. Mesh figures

Number of nodes	188391
Number of elements	1038099
Number of refinement zones	0

Table- 58. cutting planes through mesh

Figure 90	Equilibrium plane
Figure 91	Traverse section

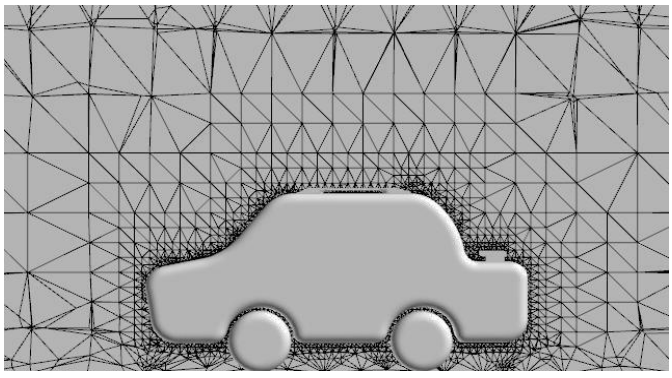

Fig -90. Flow Direction Meshing

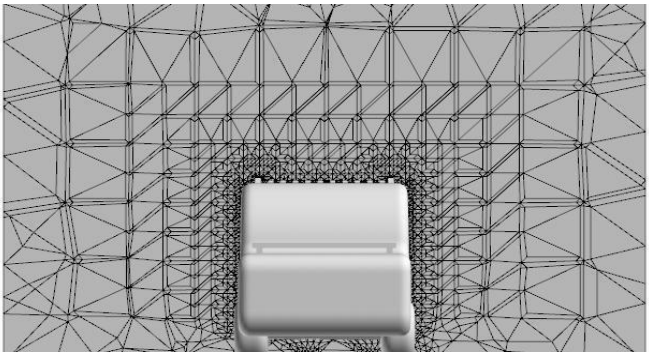

Fig- 91. Traverse Direction Meshing

4.Boundary condition & solution strategy

In this section the boundary conditions and the setup for the CFD run are listed.

Table- 59. Boundary condition

Inflow velocity	30 m/s
Outflow	Pressure outlet
Slip Walls	Top, right, left faces of wind tunnel
No-slip Walls	wind tunnel ground, body, wheels, heat-exchange

Table- 60. Solution strategy

Simulation form	"transient"
Number of time steps	10
Time rise	0.2
Physical time	2.000
Turbulence prototype	Detached Eddy Simulation
Moving ground	True
Rotating wheels	True

5.Results

In this section the results of the CFD run are reported. Table 61 gives an overview of the different result types

Table -61. Results

Table 62	Drag & lift coefficient of car
Table 63	Drag area of car
Figure 92,93,94	Pressure contours on body, Equilibrium and Traverse section plane
Figure 95	Pressure coefficient on body Face
Figure 96,97	Velocity contours on Equilibrium and horizontal cut plane
Figure 98,99	Front & side view of streamlines around body
Figure 100,101,102	Body Face y + views

Table- 62. Coefficients

Face	Drag Coefficient	Lift Coefficient
Car	0.550	0.218

Table -63. Drag areas

Face	Drag area
Car	0.67666

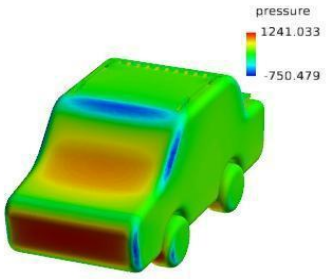

Fig- 92. Body Face pressure contour

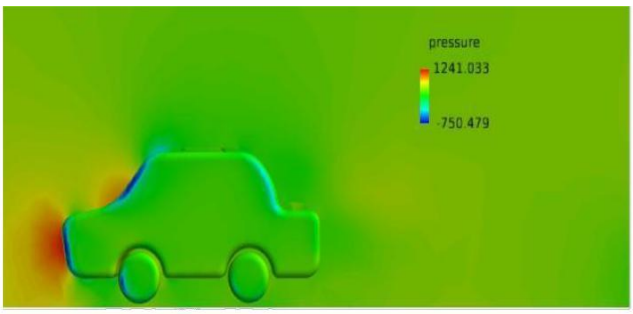

Fig -93. Mean plane pressure contour

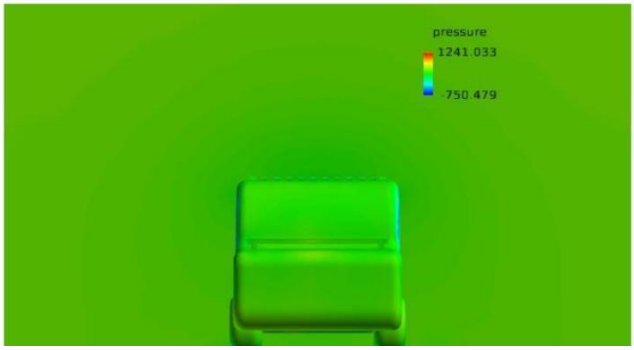

Fig -94. Traverse plane pressure contour

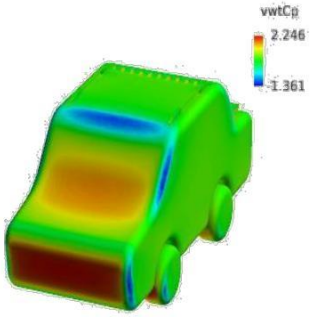

Fig- 95. Body Face pressure coefficient

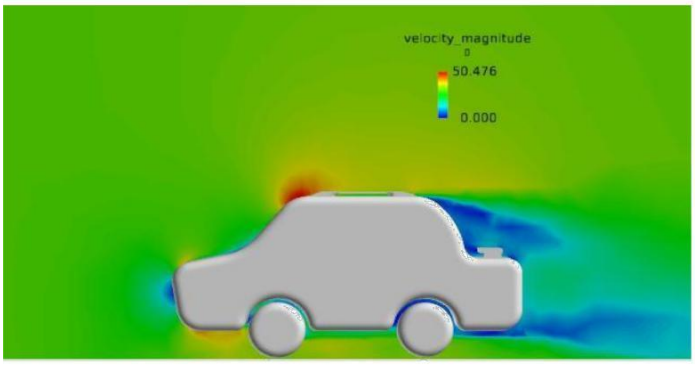

Fig -96. Mean plane velocity contour

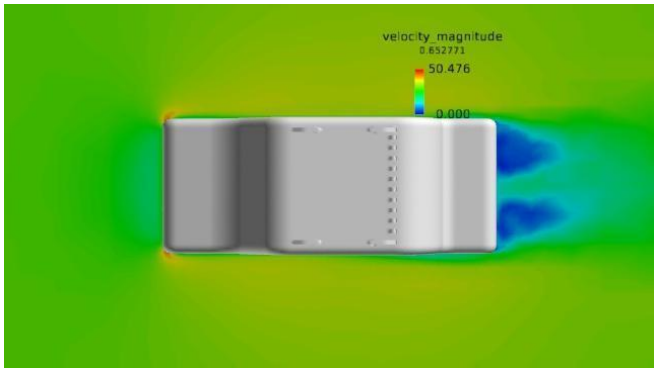

Fig- 97. Traverse plane velocity contour

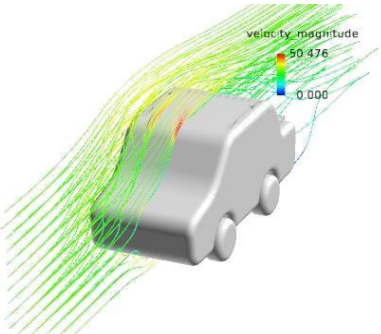

Fig- 98. Front view of streamlines

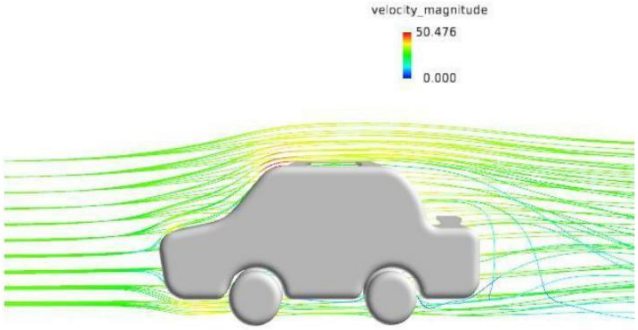

Fig- 99. Side view of streamlines

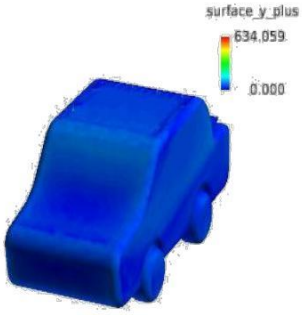

Fig -100. Body Face y + front view

Fig -101. Body Face y + Rear view

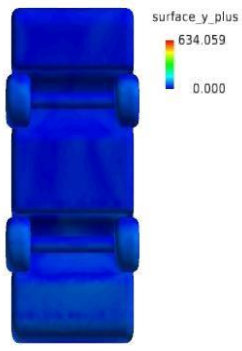

Fig -102. Body Face y + Bottom view

13. Results

Table-64. Drag and lift coeff. of baseline passenger car with a prototype fitted with spline, spoiler, tail-plate, VGs, spline and spoiler, VGs and spoiler

Configuration	Drag coefficient	% drop from base prototype	Lift coefficient	% drop From base prototype
Base Prototype	0.603	0	0.250	0
Spline	0.590	2.1	0.235	6
Spoiler	0.570	5.4	0.230	8
Tail-plate	0.595	1.3	0.240	4
VGs	0.580	3.8	0.232	7.2
Spline & spoiler	0.565	6.3	0.225	10
VGs & spoiler	0.550	8.7	0.218	12.8

In the case of SPLINE in passenger car the coefficient of drag is 0.590 and coefficient of lift is 0.230. the percentage of drop in drag coefficient in comparison of baseline car is 2.1 % and in coefficient of lift is 6%. In the case of SPOILER the coefficient of drag is 0.570 and coefficient of lift is 0.230. the percentage of drop in drag coefficient in comparison of baseline car is 5.4% and in coefficient of lift is 8%. In the Case of TAIL-PLATE in passenger car the coefficient of drag is 0.595 and Coefficient of lift is 0.240. the percentage of drop in drag coefficient in comparison of baseline car is 1.3% and in coefficient of lift is 4%. In the case of VGs in passenger car the coefficient of drag is 0.580 and coefficient of lift is 0.232. the percentage of drop in drag coefficient in comparison of baseline car is 3.8% and in coefficient of lift is 7.2%. In the case of SPLINE AND REAR SPOILER the coefficient of drag is 0.565 and coefficient of lift is 0.225. the percentage of drop in drag coefficient in comparison of baseline car is 6.3% and in coefficient of lift is 10%. In the case of VGs AND SPOILER the coefficient of drag is 0.550 and coefficient of lift is 0.218 . the percentage of drop in drag in comparison of baseline car is 8.7% and in coefficient of lift is 12.8%. Hence drag force & lift force on the passenger car is reduced as relative to drag coefficient and lift coefficient respectively. The comparative outcome between the baseline car and car with splines , spoiler , Tail-plate , VGs, splines and spoiler, VGs and spoiler are shown in table 64.

14.Conclusion

The effects of special aerodynamic add-on devices on flow and its arrangement over a passenger car may be analyzed using CFD approach. The purpose is to diminish aerodynamic drag acting on the vehicle and thus recover the fuel efficiency of passenger car. As we see the value of percentage drop of drag and lift coefficient after analysis is least by using tail-plate 1.3% and 4% going through the ascending order we got utmost percentage drop of drag force and lift force 8.7% and 12.8% by attaching VGs & spoiler on same car Hence, the drag force can be reduced by using add-on devices on vehicle and fuel economy, stability of a passenger car can be improved.

ACKNOWLEDGEMENT

we would like to express our sincere gratitude to our advisor Asst. Prof. Vishal shukla for the continuous support of our research, for his patience, motivation, enthusiasm, and immense knowledge. His guidance helped us in all the time of research.

References

[1] Pramod Nari Krishnani (2009) CFD STUDY OF DRAG REDUCTION OF A GENERIC SPORT UTILITY VEHICLE, Thesis , mechanical engineering department, California state university, Sacramento.

[2] Bhagirathsingh H Zala, Harilal S Sorathia, Dinesh L. Suthar,Vashant K. Pipalia COMPARATIVE ASSESSMENT OF DRAG FORCE OF SEDAN CAR PROTOTYPE BY COMPUTATIONAL FLUID DYNAMICS AND EXPERIMENTAL METHOD, Zala et al., International Journal of Advanced Engineering Technology E-ISSN 0976-3945, Research paper

[3] Shashank Arya, Pankaj Goud, Shubham Mathur, Vishal Sharma, Sourabh Tripathi, Vishal Shukla (2016) , A Review on "Reduction of Drag Force using ADD-ON Devices" , International Research Journal of Engineering and Technology (IRJET), Volume: 03 Issue: 11 | Nov -2016.

[4] R. B. Sharma, Ram Bansal (2013) CFD Simulation for Flow over Passenger Car Using Tail Plates for Aerodynamic Drag Reduction, IOSR Journal of Mechanical and Civil Engineering (IOSR-JMCE), Volume 7, Issue 5.

[5] Vishal Shukla, Gaurav Saxena (2015) Computational Drag Analysis of Passenger Car Using Splines and Spoiler International Journal of Engineering Trends and Technology (IJETT) – Volume 21 Number 1.